



# Microfluidic derivatisation technique for determination of gaseous molecular iodine with GC–MS

Xiaobing Pang<sup>a,b,\*</sup>, Lucy J. Carpenter<sup>a,c</sup>, Alastair C. Lewis<sup>a,c</sup>

<sup>a</sup> Wolfson Atmospheric Chemistry Laboratories, Department of Chemistry, University of York, York YO10 5DD, UK

<sup>b</sup> Key Laboratory for Aerosol-Cloud-Precipitation of China Meteorological Administration, Nanjing University of Information Science and Technology, Nanjing 210044, China

<sup>c</sup> National Centre for Atmospheric Science, University of York, York YO10 5DD, UK

## ARTICLE INFO

### Article history:

Received 28 October 2014

Received in revised form

27 January 2015

Accepted 31 January 2015

Available online 10 February 2015

### Keywords:

Microfluidic derivatisation technique

GC–MS

Gaseous molecular iodine

Ozonolysis

Iodide

## ABSTRACT

Gaseous molecular iodine ( $I_2$ ) is an important source of reactive iodine in the marine atmosphere, but the sources of  $I_2$  are not well understood due to the lack of an easily accessible, sensitive and robust technique for analysis. In this study a microfluidic derivatisation technique combined with GC–MS has been developed to measure gaseous  $I_2$ . Good linearity in the range of 0.2–416 ppb and low detection limits varying from 6 to 25 ppt for different derivatisation reagents have been achieved, which is a substantial improvement in sensitivity compared with the spectrophotometric method (detection limit of 1.20 ppb) in our previous study [L.J. Carpenter, S.M. MacDonald, M.D. Shaw, R. Kumar, R.W. Saunders, R. Parthipan, J. Wilson, J.M.C. Plane, *Nature Geoscience*, 6 (2013) 108–111]. The microfluidic technique was employed to quantify  $I_2$  produced from the heterogeneous reactions of potassium iodide solution and ozone. Good agreement was observed between the results of the microfluidic technique and the simulation of a coupled surface water–air kinetic model in the amount of  $I_2$  produced on the ozonolysis of iodide solutions.

© 2015 The Authors. Published by Elsevier B.V. This is an open access article under the CC BY license (<http://creativecommons.org/licenses/by/4.0/>).

## 1. Introduction

Gaseous  $I_2$  is a key source of iodine atoms in the marine boundary layer (MBL) [1]. Atomic iodine reacts rapidly with atmospheric  $O_3$  and the subsequent photochemical cycling results in a reduction in tropospheric  $O_3$  levels [2]. Iodine is also believed to be a source of ultrafine particles in the MBL [3], which can grow to larger particles that contribute to cloud condensation nuclei (CCN) [4] and can potentially influence global climate. Since iodine chemistry was observed to have a significant and extensive influence on photochemical  $O_3$  loss in the tropical Atlantic MBL [5], there has been increasing interest in its sources and atmospheric chemistry. The heterogeneous reaction between aqueous iodide ( $I^-$ ) and gaseous  $O_3$  was recently postulated to be the main source of oceanic  $I_2$  and hypiodous acid (HOI) through a series of laboratory experiments [1]. This hypothesis needs to be further verified in the marine atmosphere, but such evaluation is hindered by the lack of sensitive, readily accessible and robust analytical techniques to measure inorganic iodine gases at low concentrations.

Atmospheric  $I_2$  is typically measured by long-path differential optical absorption spectroscopy (LP-DOAS) [6,7]. This technique provides concentrations averaged over a path length of several kilometres and has detected  $I_2$  mixing ratios in iodine-rich coastal regions [7] with a detection limit of 0.5 ppt but is unsuitable for point measurements. Broadband cavity enhanced absorption spectroscopy (BBCEAS) can measure gaseous  $I_2$  in situ and features a significantly higher spatial resolution (less than 1 m) [8]. Combined with good temporal resolution (several minutes) BBCEAS thus complements LP-DOAS in point measurement of tropospheric  $I_2$ . Recently, atmospheric pressure chemical ionisation tandem mass spectrometry (APCI-MS)<sup>2</sup> has been successfully applied to measure gaseous  $I_2$  at low ppt levels in oceanic air at the Cape Verde Atmospheric Observatory [9]. The techniques discussed above are technically demanding and unavailable to the majority of laboratories. In recent years the diffusion denuder has been widely employed to measure gaseous  $I_2$  since this technique has the advantage of being straightforward, specific, relatively cheap and portable [10,11]. However, the technique requires several hours of field sampling and involves a series of processes including the denuder preparation, solvent elution, pre-concentration of sample solution and offline analysis by GC–MS [10,12] or a UV/vis spectrophotometer [11]. These labour intensive and complicated processes mean that avoidance of secondary contamination into the samples is a considerable challenge.

\* Corresponding author. Tel.: +44 1904 324758.

E-mail address: [pangxbyuanj@gmail.com](mailto:pangxbyuanj@gmail.com) (X. Pang).

The development of a methodology for gaseous  $I_2$  analysis which can both eliminate the laborious bench processes for sample preparation and utilise the universality of standard analytical techniques could allow more routine analysis of  $I_2$  in the environment and much-needed knowledge on its atmospheric concentrations and distributions. In this work, a rapid, simple and sensitive microfluidic derivatisation approach for  $I_2$  analysis has been developed utilising accelerated and highly efficient derivatisation reactions inside a micro-reactor. This methodology for gaseous  $I_2$  builds on our previous reported microfluidic technique [13,14]. The performance of the microfluidic derivatisation technique for  $I_2$  analysis was evaluated through measurement of  $I_2$  emitted from the interface of aqueous  $I^-$  and  $O_3$ . The observations were compared with the simulations using a coupled surface liquid–air box model [1].

## 2. Materials and methods

### 2.1. Chemicals

All chemicals were purchased from Sigma-Aldrich Company. Solvent methanol (HPLC grade) was bought from Fisher (UK). N, N-dimethylaniline (NDMA), 1,3,5-trimethoxybenzene (TMB), 2,6-dimethylphenol (DMP) were directly utilised as derivatisation reagents. Ultrapure water was provided by the water purification equipment (ELGA-PURELAB flex system, VEOLIA, France).

### 2.2. Micro-reactor layout and experimental set-up for gaseous $I_2$ measurement

The modular glass microfluidic chip was fabricated by Dolomite Centre, UK. The detailed description of the micro-reactor layout can be seen in our previous work [13,14]. The micro-reactor integrates three key functions: (1) a gas and liquid reactor, (2) sample pre-concentration, and (3) reagent heating. The  $I_2$  sample gases passed into the micro-reactor at  $200\text{ mL min}^{-1}$  through inlet 2 and inlet 3 and was helped by a new KNF diaphragm gas pump (PM20994-022, Neuberger, Germany), which is located at the outlet of the sample impinger. The derivatisation solution was introduced into the micro-reactor simultaneously at  $60\text{ }\mu\text{L min}^{-1}$  through inlet 1 by a peristaltic pump (Watson Marlow 205S, UK). The sample gas and the solution of derivatisation reagent mix together through the mixing junctions and react in the micro-channel. The reaction solution eluting from the micro-reactor was collected into a sample impinger. The detailed experimental set-up is shown in Fig. 1. About 1.0 mL derivative solution can be obtained after 30 min reaction and further pre-

concentrated to  $50\text{ }\mu\text{L}$  by a nitrogen flow, prior to GC–MS measurement.

### 2.3. Generation of standard gaseous $I_2$

Gaseous  $I_2$  standards were generated using a commercial molecular iodine permeation tube (Kin-TekTM, USA) stored in a permeation oven at  $40\text{ }^\circ\text{C}$ . Iodine emission rates at the operating temperatures were determined directly by repeated weighing of the tube at four week intervals. The permeation chamber was flushed with zero grade nitrogen (BOC) at a flow rate of  $50\text{ mL min}^{-1}$ . The outlet flow was further diluted with a nitrogen flow varying in the range of  $0\text{--}10.0\text{ L min}^{-1}$  in order to achieve the desired concentration of gaseous  $I_2$ . Where required, a needle valve and T-piece was used to ensure that the flow rate of standard  $I_2$  gas remained constant. The experimental set-up is shown in Fig. 1. All flows were exactly controlled to remain constant by mass flow controllers (MKS, UK), which were all calibrated by an air flow calibrator (Gilian Gilibrator-2, Sensidyne, USA). The range of gaseous  $I_2$  concentrations obtainable was  $0.2\text{--}22\text{ ppb}$ . To minimise the wall losses and photo-degradation of iodine, all tubing and fittings were wrapped in aluminium foil and heated tape to keep the temperature at  $60\text{ }^\circ\text{C}$ .

### 2.4. GC–MS conditions

Separation and detection of the iodine derivatives were performed on a GC–MS (Perkin-Elmer, USA) with quadrupole MS and a DB5 column ( $30\text{ m} \times 0.25\text{ mm} \times 1.0\text{ }\mu\text{m}$ , length  $\times$  internal diameter  $\times$  film thickness). GC conditions were as follows: the oven temperature was initially set at  $80\text{ }^\circ\text{C}$  for 1 min, ramped to  $230\text{ }^\circ\text{C}$  with a temperature ramp of  $30\text{ }^\circ\text{C min}^{-1}$  and then held at  $230\text{ }^\circ\text{C}$  for 1 min. The temperatures of the GC inlet and GC–MS transfer line were kept at  $250\text{ }^\circ\text{C}$ . The GC–MS conditions were same for the NDMA, TMB, and DMP derivatives. The mass spectrometer was operated in scan mode with a mass range of  $100\text{--}300\text{ Da}$  to identify the most abundant ions of the iodine derivatives. The select ion chromatograms of most abundant ions were used to quantify the derivative concentrations.

### 2.5. Collection efficiency and reproducibility

To evaluate the collection efficiency (CE) of the microfluidic derivatisation technique for gaseous  $I_2$ , a series of  $I_2$  gases in different concentrations were passed through a small downstream vial filled with  $1.0\text{ mL}$  of the derivatisation solution in series after passing out from the sample impinger. The collection efficiency was calculated as CE% using  $100\% \times (1 - A_v/A_i)$ , where  $A_v$  and  $A_i$  are the amounts of iodine collected in the vial and the impinger, respectively. The

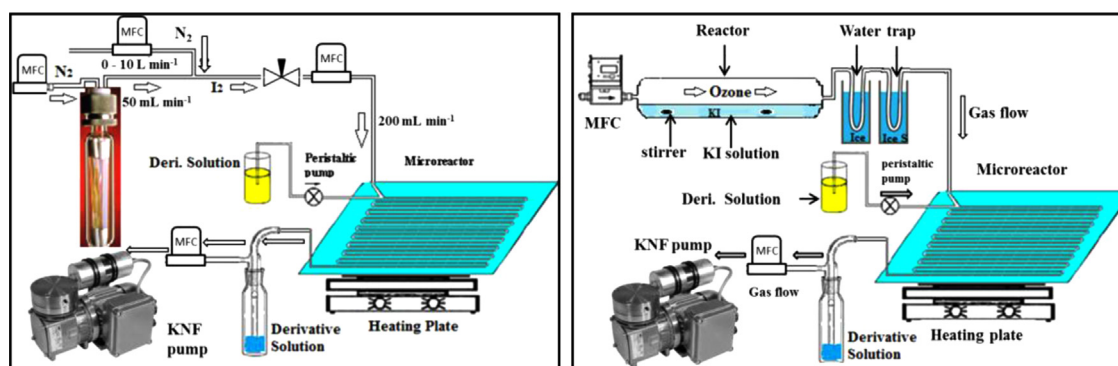


Fig. 1. Schematics of microfluidic derivatisation system for gaseous  $I_2$  produced from permeation tubing (Left panel) and for the determination of  $I_2$  from the KI and  $O_3$  reaction (Right panel).

reproducibility of the microfluidic derivatisation technique was determined by the replicate analyses ( $n=5$ ) of standard  $I_2$  gases at three different concentrations under the same experimental conditions. The reproducibility was expressed as the relative standard deviation (RSD)=[(standard deviation of observed concentration)/(average of observed concentration)]  $\times 100\%$ .

## 2.6. Measurement of gaseous $I_2$ emitted from ozonised KI solution

The microfluidic derivatisation technique was employed to measure gaseous  $I_2$  from the heterogeneous reaction of aqueous KI and  $O_3$ , which occurred in a cylinder glass reaction vessel (36 cm length  $\times$  5.56 cm radius). Iodide solutions ( $10^{-6}$ – $10^{-5}$  mol L $^{-1}$  KI), whose concentrations are close to those at seawater surface ( $[I^-]$   $10^{-7}$ – $10^{-6}$  mol L $^{-1}$ ) [15] were prepared from phosphate-buffered water at variable pHs and stored in an amber volumetric bottles at 4 °C. The  $O_3$  flow over iodide solution (200 mL) was maintained at 200 mL min $^{-1}$ .  $O_3$  was produced from dry hydrocarbon-free air by its exposure to a UV lamp in an  $O_3$  generator (Part no. 97-0067-02, UVP) and the  $O_3$  mixing ratio  $[O_3]$  was controlled in the range 25–250 ppb by adjusting the length of UV lamp exposed to air. The  $[O_3]$  were monitored by a model 49i ozone monitor (Thermo Scientific, USA). The above experimental conditions were identical to those in our previous experiment, which is favourable to the comparison between the microfluidic technique and the spectrophotometric method employed in our previous study. During the experiment the entire reaction vessel was covered with aluminium foil to prevent  $I_2$  losses from photolysis. The gas from the outlet of the reaction vessel then passed through two cold traps in series (one at 0 °C and another at  $-10$  °C) to remove the water and was drawn into the micro-reactor to react with the derivatisation reagents (NDMA, TMB, and DMP), respectively. The resulting derivative solution was collected in 10 ml impinger whose outlet was collected by a KNF diaphragm gas pump (PM20994-022, Neuberger, Germany) to keep the gas–liquid flow fluent from microreactor. The gas flow of KNF pump was set at 250 mL min $^{-1}$  by a mass flow controller to avoid an extreme low vacuum in the impinger. The final resulting solution (about 1.0 mL) was pre-concentrated to 50  $\mu$ L by nitrogen flow and then determined by GC–MS. The schematic of the whole experimental set-up is shown in Fig. 1.

## 2.7. Modelling iodine emissions

A commercial modelling programme FACSIMILE (MCPA Software) was used to simulate the gaseous  $I_2$  emission from KI solution using a series of chemical reactions involved in interfacial aqueous iodine dynamics, including iodide oxidation, iodine disproportionation, and iodine reduction. Iodine production was initiated by the gas phase flux of  $O_3$  into the interfacial layer containing fixed  $[I^-]$ . The interfacial layer was treated as a box, assuming no horizontal advection but mixing vertically with bulk mixed-layer water at a fixed interfacial layer turnover time. A detailed description of the model is given in Carpenter et al. [1].

## 3. Results and discussions

### 3.1. Optimisation process

NDMA [10], TMB [12] and DMP [16] have been reported to be effective derivatisation reagents for  $I_2$  in previous publications and thus were chosen in this study. According to our previous experience, the concentration of derivatisation reagents, the solvent, microchip temperature, flow rates of gas and solution, and the reaction time can all affect the reaction efficiency and

**Table 1**

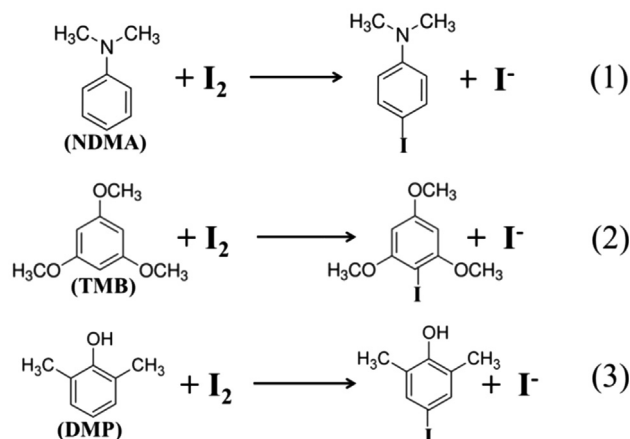
Optimal experimental conditions for  $I_2$  microfluidic derivatisation reaction.

Concentration of derivatisation reagent	Temperature (°C)	Flow rate of iodine gas (mL min $^{-1}$ )	Flow rate of solution ( $\mu$ L min $^{-1}$ )	Solvent
$1 \times 10^{-3}$ mol L $^{-1}$	60	200	60	Methanol

reproducibility of the derivatisation reaction and an optimisation process of the parameters is required to achieve the highest efficiency of derivatisation from each micro-preparative system. We have undertaken a similar optimisation here to that conducted previously for gaseous carbonyl measurements [13,14]. The optimal conditions for the derivatisations of gaseous  $I_2$  in microfluidic chip are shown in Table 1.

### 3.2. GC chromatograms and MS spectra of derivatives

The GC chromatogram (Fig. 2) of each derivative solution contained only one new peak and the mass spectrum of the peak is consistent with that of the derivative formed from the derivatisation reactions of NDMA, TMB, and DMP with molecular iodine; reactions (1), (2) and (3), respectively [16,17].



The selected ion chromatograms of the most abundant ions with  $m/z=119$ , 121 and 137 Da for the derivatives of NDMA, DMP and TMB, respectively, in the mass spectra (Fig. 2) were used to quantify the derivative concentrations in solutions.

### 3.3. Method calibrations and detection limits

The method calibration curves for the microfluidic derivatisation technique were established by measuring a series of gaseous  $I_2$  of different concentrations prepared by the nitrogen dilution of  $I_2$  gas emitted from the permeation system under the optimal conditions of micro-reactor (Fig. 1). As Fig. 3a shows, three derivatisation reagents show good linearity on the measurement of gaseous  $I_2$  varying from 0.2 to 22 ppb. The linear equations for  $I_2$  among the three reagents are different in intercepts and gradients.

Above calibration curves are suitable for the measurement of gaseous  $I_2$  with its mixing ratio less than 22 ppb. In some cases the microfluidic technique will be employed to measure some gaseous  $I_2$  higher than 22 ppb. Therefore, another calibration method based on the standard solutions of iodine derivatives of NDMA, TMB and DMP at different concentrations was developed to perform the task. In this method the concentrations of iodine derivative solutions have been transferred into the mixing ratios of gaseous iodine assuming the iodine derivatives are formed by

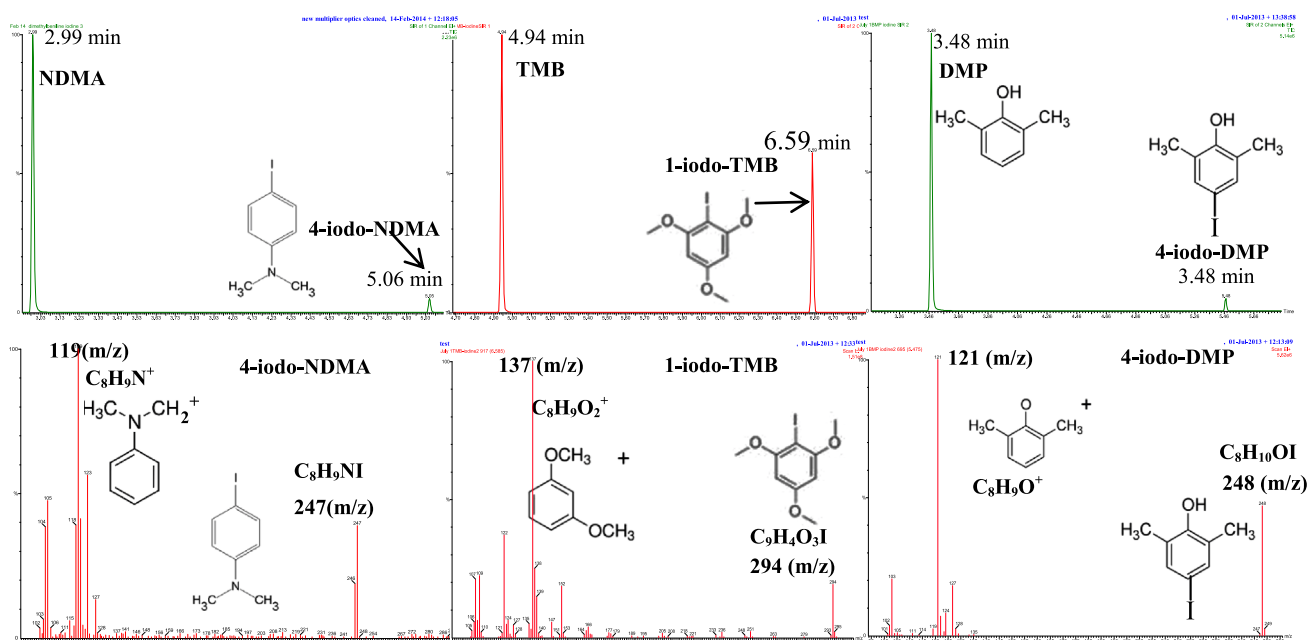


Fig. 2. GC chromatograms of the derivatives and derivatisation reagents (NDMA, TMB, and DMP) (Panels on above row) and mass spectra of the derivatives (panels on low row).

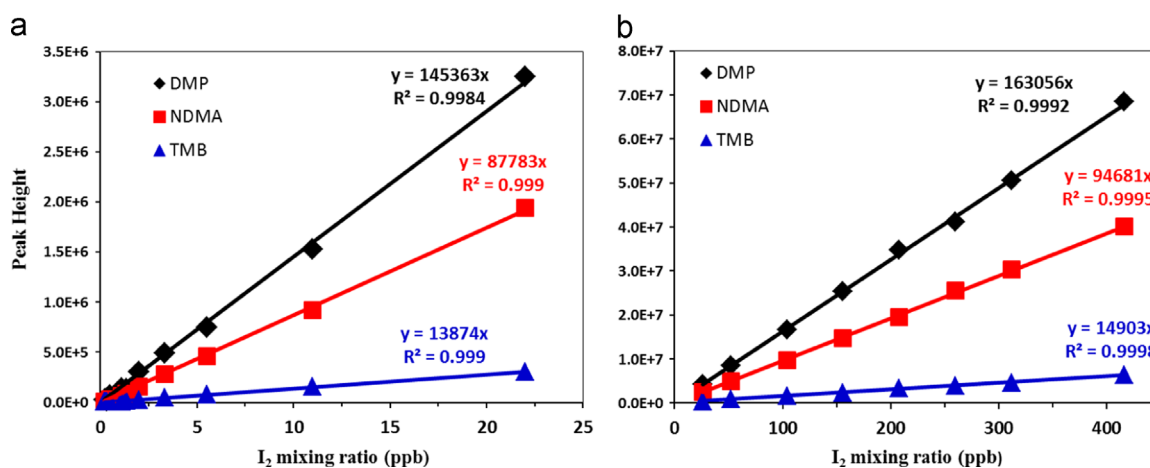


Fig. 3. Calibration curves of iodine derivatives of NDMA, TMB and DMP. (a) Calibrations are based on the derivatisations of standard gaseous  $I_2$  and DMP, NDMA, and TMB, respectively. (b) Calibrations are based on the standard solutions of DMP, NDMA, and TMB derivatives, respectively.

gaseous  $I_2$  and derivatisation reagents at 100% reaction efficiencies. As Fig. 3b shows, the gradients of the calibration curves based on standard solutions are higher than those based on gaseous  $I_2$  derivatisations by 11.5%, 7.9% and 7.4% for DMP, NDMA and TMB, respectively, which may be caused by the lower actual derivatisation efficiencies in micro-reactor than those assumed to be 100% in the standard calibration solutions. The differences in gradient are less than the instrumental errors (15%). Thus, it can be considered that no systemic differences exist in the calibration equations between the standard calibration solutions and gaseous iodine derivatisation, which implies that the calibration solution method is suitable for gaseous  $I_2$  determinations.

Since no signal can be directly observed in the blank samples, we use the standard calculation of the Limit of Detection (LOD) to express the sensitivity of the microfluidic technique. The LOD is determined by the derivative signal which is 8 times higher than the noise ( $S/N=8$ ) in the GC–MS chromatogram. The LODs for gaseous  $I_2$  are calculated to be 6 ppt, 12 ppt and 25 ppt by DMP, TMB and NDMA derivatisations, respectively, for 30 min sampling.

Table 2

Collection efficiency (CE) and reproducibility of the microfluidic derivatisation technique to gaseous  $I_2$ .

[ $I_2$ ] (ppbv)	CE (%) <sup>a</sup>			Reproducibility(%) <sup>b</sup>		
	DMP	NDMA	TMB	DMP	NDMA	TMB
22	94 ± 6	95 ± 4	97 ± 3	6.5	4.3	4.6
11	95 ± 3	96 ± 5	96 ± 2	4.5	5.0	4.2
1.1	98 ± 2	97 ± 3	97 ± 2	3.5	4.4	4.0

<sup>a</sup> CE% using  $100 \times (1 - A_v/A_t)$ , ( $n=5$ ).

<sup>b</sup> RSD of replicate analyses ( $n=5$ ).

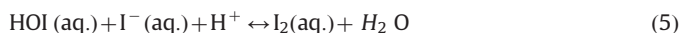
These LODs are close to typical concentrations of gaseous  $I_2$  observed above seawater [9].

Collection efficiency (CE) and reproducibility for gaseous  $I_2$  at three mixing ratios are shown in Table 2. All result data indicate that the microfluidic derivatisation technique for gaseous  $I_2$  is satisfactory in CE and reproducibility.



### 3.4. Application in gaseous $I_2$ measurement

The microfluidic derivatisation technique was employed to determine gaseous  $I_2$  emitted from the ozonised KI aqueous solution to test the performance of the technique for time resolved measurements. The gaseous  $I_2$  emissions measured by the microfluidic technique through the three derivatisation reagents in Fig. 4 increase near linearly with both  $[O_3]$  and  $[I^-]$ , which is consistent with the observation of previous study [1]. The consistence indicates that the microfluidic derivatisation technique is suitable for the quantification of gaseous  $I_2$ . The similar results obtained from DMP, NDMA and TMB derivatisations imply the derivatisation reagents are all feasible and show the same performance for gaseous  $I_2$  derivatisation during the employment of the microfluidic technique. The microfluidic derivatisation measurements of gaseous  $I_2$  emission were compared with the liquid–air model simulations during a series of experiments to investigate the effects of  $[O_3]$  and  $[I^-]$  on  $I_2$  emission rate. As Fig. 4 shows, the comparisons imply the measurements of the microfluidic technique on gaseous  $I_2$  below 200 ppb are consistent with the model simulations. As the gaseous  $I_2$  concentration increases the discrepancy between the two methods gradually widens. The results obtained from the microfluidic technique were lower by 13.3–30.8% than the model simulations when the mixing ratio of gaseous  $I_2$  are higher than 50 ppb. It has been established that gaseous  $I_2$  is produced from the reaction between  $O_3$  gas and aqueous  $I^-$  via the following basic mechanism:



There are four potential reasons for the widen gaps between two methods, which are: (1) the low reaction efficiencies of microfluidic derivatisation to gaseous  $I_2$  at high mixing ratios, (2) dissolution of gaseous  $I_2$  in water contained in the cold traps, (3) the wall loss of gaseous  $I_2$  on tubing and glassware, and (4) processes occurring at high iodine concentrations which are not included in the model. It should be noted that the  $I_2$  losses cannot be quantified using the method in Section 2.5 at high  $I_2$  concentrations since the concentrations of the standard  $I_2$  gas were less than 22 ppb. Hypoiodous acid (HOI) is in equilibrium with  $I_2$  (Eq. (5)) with an HOI/ $I_2$  ratio of less than 0.1 at  $10^{-5}$  M  $[I^-]$  solution (pH 8) and about 500 in sea water ( $10^{-7}$ – $10^{-8}$  M  $[I^-]$ ) [1]. The HOI production can result in the less  $I_2$  emission from aqueous solution, which leads to the lower qualifications by the microfluidic technique than those by modelling expectations.

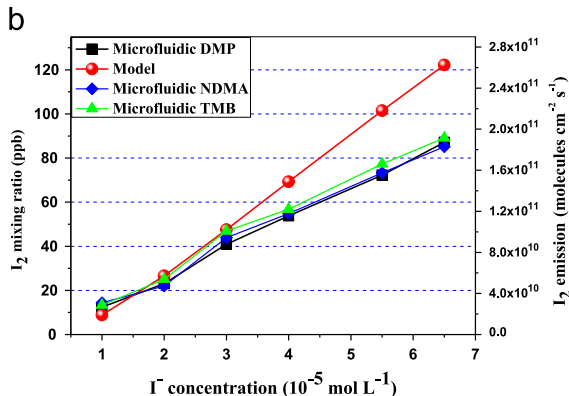
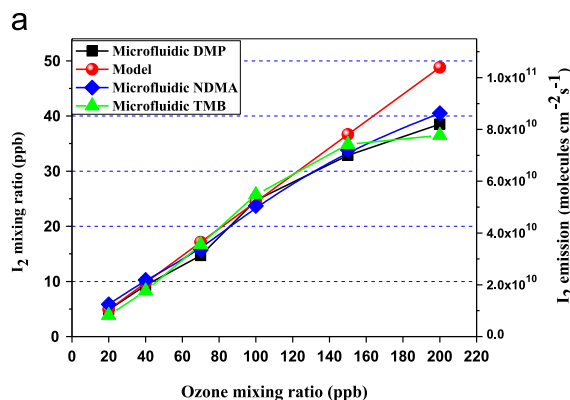


Fig. 4. Comparison between the microfluidic derivatisation technique and model simulation of the effects of  $[O_3]$  and  $[I^-]$  on gaseous  $I_2$  emission. Experimental conditions for the  $O_3$  effects:  $1.5 \times 10^{-5}$  mol  $L^{-1}$  KI, pH=8.0. Effect of  $I^-$  concentration:  $[O_3]$  70 ppb, pH=8.0.

The linear dependence of gaseous  $I_2$  production on  $[O_3]$  and  $[I^-]$  in this study are consistent with the phenomena observed in previous studies [1,18,19]. Carpenter et al. [1] showed that the emission rate of gaseous  $I_2$  depends primarily on the  $O_3$  flux into the interfacial layer, the surface  $[I^-]$ , acidity, and mixing of the interfacial layer into bulk water. Due to little competition for  $O_3$  other than reaction with  $I^-$ ,  $I_2$  production is essentially linear with  $[O_3]$ . Both  $O_3$  uptake and  $O_3$  accumulation in the interfacial layer increase with  $[I^-]$ , thus the net result is a near-linear dependence of  $I_2$  production on  $[I^-]$ .

The microfluidic derivatisation technique was utilised to investigate the influence of pH on the gaseous  $I_2$  emission from ozonised KI solution. As Fig. 5 shows, the results from the three derivatisation reactions imply that  $I_2$  yields are markedly higher at pH < 4 (pH=2, 3 and 4), remain stable between pH 5 and pH 10, then dropping dramatically to near zero from pH 11 to pH 12. This phenomenon is consistent with the observations in previous reported studies [19,20]. The enhancement of gaseous  $I_2$  production when using acidic KI (aq.) can be explained by reaction (4) and (5), where  $H^+$  is necessary to generate  $I_2$  and high  $[H^+]$  is favourable to  $I_2$  formation [19].

### 4. Conclusions

A new and near automated microfluidic lab-on-a-chip derivatisation technique has been developed for the sensitive measurement of gas-phase molecular iodine ( $I_2$ ) and has been tested in a series of heterogeneous reactions of KI solution and ozone. The microfluidic derivatisation technique for gaseous  $I_2$  analysis can both eliminate the laborious bench processes for sample

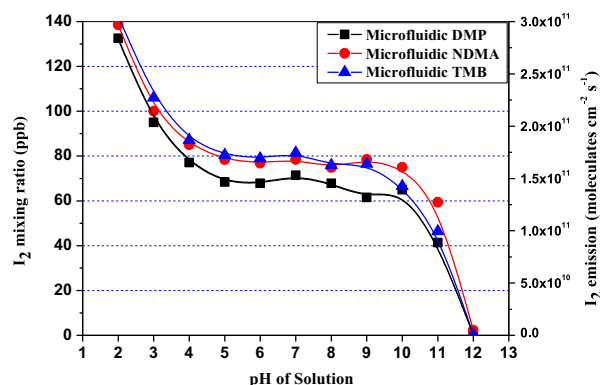


Fig. 5. Microfluidic derivatisation technique employed to study the effect of pH on gaseous  $I_2$  emission.  $[O_3]$ : 150 ppb,  $[I^-]$ :  $3.0 \times 10^{-5}$  mol  $L^{-1}$ .

preparation and utilise the universality of standard analytical instrument (GC–MS), which could allow more routine analysis of  $I_2$  in the environment. The consistency in  $I_2$  production dependency on  $[I^-]$  and  $[O_3]$  between the microfluidic derivatisation technique and the simulation of a coupled surface water–air kinetic model provides some initial evidence for the effectiveness of the technique in practical application. The low detection limits varying from 6 to 25 ppt for different derivatisation reagents have been achieved, which is a substantial improvement in sensitivity compared with the spectrophotometric method. Since the detection limits of microfluidic derivatisation technique are close to many reported tropospheric mixing ratios, the microfluidic derivatisation technique could be employed for ambient  $I_2$  measurements with time resolution of 30 min or less.

## Acknowledgement

XP gratefully thank the National Natural Science Foundation of China (NSFC) (Grants 41322035 and 41175110) for financial support. All authors acknowledge the support from Natural Environment Research Council (NERC) of UK (Grant no. NE/F015240/1). Many thanks to Tomas Sherwen for experimental assistances and to Rosie J. Chance for helpful discussions.

## References

- [1] L.J. Carpenter, S.M. MacDonald, M.D. Shaw, R. Kumar, R.W. Saunders, R. Parthipan, J. Wilson, J.M.C. Plane, *Nat. Geosci.* 6 (2013) 108–111.
- [2] A. Saiz-Lopez, J.M. Plane, A.R. Baker, L.J. Carpenter, R. von Glasow, J.C. Gómez Martín, G. McFiggans, R.W. Saunders, *Chem. Rev.* 112 (2011) 1773–1804.
- [3] C.D. O'Dowd, P. Aalto, K. Hmeri, M. Kulmala, T. Hoffmann, *Nature* 416 (2002) 497–498.
- [4] G. McFiggans, C. Bale, S. Ball, J. Beames, W. Bloss, L. Carpenter, J. Dorsey, R. Dunk, M. Flynn, K. Furneaux, *Atmos. Chem. Phys.* 10 (2010) 2975–2999.
- [5] K.A. Read, A.S. Mahajan, L.J. Carpenter, M.J. Evans, B.V.E. Faria, D.E. Heard, J.R. Hopkins, J.D. Lee, S.J. Moller, A.C. Lewis, L. Mendes, J.B. McQuaid, H. Oetjen, A. Saiz-Lopez, M.J. Pilling, J.M.C. Plane, *Nature* 453 (2008) 1232–1235.
- [6] A. Saiz-Lopez, J.A. Shillito, H. Coe, J.M.C. Plane, *Atmos. Chem. Phys.* 6 (2006) 1513–1528.
- [7] A. Saiz-Lopez, J.M.C. Plane, *Geophys. Res. Lett.* 31 (2004) L04112.
- [8] A. Saiz-Lopez, J.M.C. Plane, G. McFiggans, P.I. Williams, S.M. Ball, M. Bitter, R.L. Jones, C. Hongwei, T. Hoffmann, *Atmos. Chem. Phys.* 6 (2006) 883–895.
- [9] M.J. Lawler, A.S. Mahajan, A. Saiz-Lopez, E.S. Saltzman, *Atmos. Chem. Phys.* 14 (2014) 2669–2678.
- [10] R.-J. Huang, X. Hou, T. Hoffmann, *Environ. Sci. Technol.* 44 (2010) 5061–5066.
- [11] R.J. Chance, M. Shaw, L. Telgmann, M. Baxter, L.J. Carpenter, *Atmos. Meas. Tech.* 3 (2010) 177–185.
- [12] R.J. Huang, T. Hoffmann, *Anal. Chem.* 81 (2009) 1777–1783.
- [13] X. Pang, A.C. Lewis, M. Ródenas-García, *J. Chromatogr. A* 1296 (2013) 93–103.
- [14] X. Pang, A.C. Lewis, A.R. Rickard, M.T. Baeza-Romero, T.J. Adams, S.M. Ball, M.J. S. Daniels, I.C.A. Goodall, P.S. Monks, S. Peppe, M. Ródenas García, P. Sánchez, A. Muñoz, *Atmos. Meas. Tech.* 7 (2014) 373–389.
- [15] R. Chance, A.R. Baker, L. Carpenter, T.D. Jickells, *Environ. Sci.: Process. Impacts* 16 (2014) 1841–1859.
- [16] H.S. Shin, Y.S. Oh-Shin, J.H. Kim, J.K. Ryu, *J. Chromatogr. A* 732 (1996) 327–333.
- [17] R.J. Huang, T. Hoffmann, *J. Chromatogr. A* 1210 (2008) 135–141.
- [18] J.A. Garland, H. Curtis, *J. Geophys. Res.: Ocean.* 86 (1981) 3183–3186.
- [19] Y. Sakamoto, A. Yabushita, M. Kawasaki, S. Enami, *J. Phys. Chem. A* 113 (2009) 7707–7713.
- [20] S. Hayase, A. Yabushita, M. Kawasaki, S. Enami, M.R. Hoffmann, A.J. Colussi, *J. Phys. Chem. A* 114 (2010) 6016–6021.